Available online at www.sciencedirect.com

ScienceDirect

IFAC Papers Online CONFERENCE PAPER ARCHIVE

IFAC-PapersOnLine 49-10 (2016) 171–176

Dynamics of Heterogeneous Connected Vehicle Systems

Nan I. Li and Gábor Orosz

Department of Mechanical Engineering,
University of Michigan, Ann Arbor, MI, 48109, USA
(e-mail: nanli@umich.edu, orosz@umich.edu)

Abstract: In this paper, we propose a method to analyze the longitudinal dynamics of heterogeneous connected vehicle systems including human-driven vehicles and vehicles driven by connected cruise control. Human reaction time and digital sampling time are incorporated in the models. Conditions of plant stability and head-to-tail string stability are presented.

Keywords: vehicle-to-vehicle (V2V) communication, heterogeneity, time delay, string stability

1. INTRODUCTION

Advanced driver assistance systems (ADAS) have been used to improve vehicle safety and passenger comfort in the last couple of decades. Vehicle-to-vehicle (V2V) communication has the potential to further enhance the performance of these systems by allowing the vehicle to monitor a larger traffic environment; see (Kianfar et al., 2012), (di Bernardo et al., 2015), and (Alam et al., 2015). Recently, connected cruise control (CCC) was proposed to regulate the longitudinal motion of vehicles, which exploits V2V information broadcast by multiple vehicles ahead and allows high flexibility in the structure of vehicle networking; see (Orosz, 2014). While V2V-based ADAS systems are traditionally applied for platoons composed of digitally controlled vehicles, CCC can be used to improve traffic conditions even with low penetration of CCC vehicles within the human-driven traffic flow.

When mixing CCC vehicles to the flow of human-driven vehicles, a hybrid system is created since human-driven vehicles operate in continuous time, while CCC vehicles are controlled by digital controllers in discrete time. In previous works, such systems were analyzed either by converting everything into discrete time by discretizing the continuous-time dynamics (Qin et al., 2015); or by converting everything into continuous time by approximating the time-varying delay imposed by the discrete-time dynamics with constant time delay (Ge and Orosz, 2014). Both of these are approximations of the true dynamics that will be considered in this paper. In particular, we are interested in the following performance measures: plant stability and string stability. Plant stability indicates the ability of a vehicle to approach steady state when no disturbances are imposed by other vehicles. On the other hand, string stability indicates the ability of a vehicle to attenuate disturbances imposed by the vehicles ahead. String stability is typically a stronger condition and in this paper we mainly focus on string stability.

The paper is organized as follows. In Section 2, a generalized modeling framework for the longitudinal dynamics of connected vehicle systems containing human-driven vehicles and CCC vehicles is presented, together with criteria for plant stability and head-to-tail string stability. In Section 3, we derive the formulae to analyze string stability of human-driven vehicle networks, CCC vehicle networks, and general heterogeneous connected vehicle systems that contain both human-driven and CCC vehicles. In Section 4, we investigate two connected vehicle systems as case studies to validate our formulae and make some comparisons to the two approximation methods. Finally, we conclude our paper in Section 5.

2. DYNAMICS AND STABILITY

In this section, a general modeling framework for the longitudinal dynamics of human-driven vehicles and CCC vehicles is presented.

2.1 Longitudinal Dynamics of Human-driven Vehicles

We assume that a human driver can monitor the motion of the vehicle immediately ahead and respond to stimuli like the headway h, the velocity v and the velocity of the car ahead v_1 with a reaction time delay; see Fig. 1(a). We model human drivers using the continuous-time deterministic system

$$\begin{aligned} \dot{h}(t) &= v_1(t) - v(t), \\ \dot{v}(t) &= \alpha_{\rm h}\big(V(h(t-\tau)) - v(t-\tau)\big) \\ &\quad + \beta_{\rm h}\big(v_1(t-\tau) - v(t-\tau)\big), \end{aligned} \tag{1}$$

where the dot stands for differentiation with respect to time t, $\alpha_{\rm h}$ represents the gain to match the actual velocity to a distance dependent reference velocity, while $\beta_{\rm h}$ represents the gain to match the velocity to that of the vehicle ahead. Also, τ represents human reaction time, which is typically in the range 0.4∼1.0 [s]. The function $V(h)$ denotes the range policy, which gives the reference velocity as a function of the headway h. In particular, we assume the monotonically increasing range policy function

$$V(h) = \begin{cases} 0 & \text{if} \quad h \le h_{\rm st}, \\ v_{\max}\big[1 - \cos\big(\pi \frac{h-h_{\rm st}}{h_{\rm go}-h_{\rm st}}\big)\big] & \text{if} \quad h_{\rm st} < h < h_{\rm go}, \\ v_{\max} & \text{if} \quad h \ge h_{\rm go}, \end{cases} \tag{2}$$

Peer review under responsibility of International Federation of Automatic Control.
10.1016/j.ifacol.2016.07.520

which represents the driver's intention to keep a larger distance with increasing speed; see (Ge and Orosz, 2014).

In this paper we investigate dynamics in the vicinity of the equilibrium

$$h(t) \equiv h^*, \quad v_1(t) \equiv v(t) \equiv v^* = V(h^*). \tag{3}$$

One may define the perturbations

$$\tilde{h}(t) = h(t) - h^*, \quad \tilde{v}_1(t) = v_1(t) - v^*, \quad \tilde{v}(t) = v(t) - v^*, \tag{4}$$

and linearize (1) about (3) to obtain

$$\dot{x}(t) = A_{\rm h0}x(t) + A_{\rm h1}x(t-\tau) + B_{\rm h0}\tilde{v}_1(t) + B_{\rm h1}\tilde{v}_1(t-\tau), \tag{5}$$

where $x = \begin{bmatrix}\tilde{h} & \tilde{v}\end{bmatrix}^{\rm T}$ and the matrices are given by

$$A_{\rm h0} = \begin{bmatrix}0 & -1\\ 0 & 0\end{bmatrix}, \qquad A_{\rm h1} = \begin{bmatrix}0 & 0\\ \alpha_{\rm h}N & -(\alpha_{\rm h}+\beta_{\rm h})\end{bmatrix},$$
$$B_{\rm h0} = \begin{bmatrix}1\\ 0\end{bmatrix}, \qquad B_{\rm h1} = \begin{bmatrix}0\\ \beta_{\rm h}\end{bmatrix}, \tag{6}$$

and $N = V'(h^*)$ is the derivative of range policy (2) at the equilibrium. Note that (5) is a linear system with constant delay that appears both in the input and in the state.

We are interested in the longitudinal velocity of the vehicle, so we define the output

$$\tilde{v} = Cx, \qquad C = [0\ 1]. \tag{7}$$

For a linear time-invariant (LTI) system, we can use a transfer function to represent the dynamic relationship between the input and the output. Taking the Laplace transform of (5,7) with zero initial condition, we obtain

$$\tilde{V}(s) = T^{\rm h}(s)\tilde{V}_1(s) \tag{8}$$

where $\tilde{V}(s)$ and $\tilde{V}_1(s)$ represent the Laplace transform of $\tilde{v}(t)$ and $\tilde{v}_1(t)$, respectively, and the transfer function is

$$T^{\rm h}(s) = C\big(sI - A_{\rm h0} - A_{\rm h1}{\rm e}^{-\tau s}\big)^{-1}\big(B_{\rm h0} + B_{\rm h1}{\rm e}^{-\tau s}\big). \tag{9}$$

When driving the system with periodic input $\tilde{v}_1(t) = v_1^{\rm amp}\sin(\omega t)$, the steady state output becomes $\tilde{v}^{\rm ss}(t) = |T^{\rm h}({\rm j}\omega)|v_1^{\rm amp}\sin(\omega t + \measuredangle T^{\rm h}({\rm j}\omega))$, where $|\cdot|$ and $\measuredangle$ denote the magnitude and the angle of a complex number.

2.2 Longitudinal Dynamics of CCC Vehicles

We assume that a CCC vehicle can monitor the positions and velocities of multiple vehicles ahead through V2V communication and use this information to control its own motion. Fig. 1(b) shows a scenario where the CCC vehicle monitors the motion of n vehicles ahead, which may be human-driven or CCC vehicles. In particular, we assume that it monitors the headway h and the velocities $v_1, ..., v_n$. We also assume that the clocks of the connected vehicles are synchronized and no packets are dropped.

We assume that the CCC vehicle uses a similar control algorithm as the human drivers but applies a zero-order hold (ZOH). Thus, at the time interval $t \in [k\Delta t, (k+1)\Delta t)$ its dynamics is governed by

$$\begin{aligned}\dot{h}(t) &= v_1(t) - v(t),\\ \dot{v}(t) &= u\big((k-1)\Delta t\big),\\ u(t) &= \alpha\big(V(h(t)) - v(t)\big) + \sum_{i=1}^{n}\beta_i\big(v_i(t) - v(t)\big),\end{aligned} \tag{10}$$

where α is the gain for the difference between the velocity and the reference velocity given by range policy (2), while

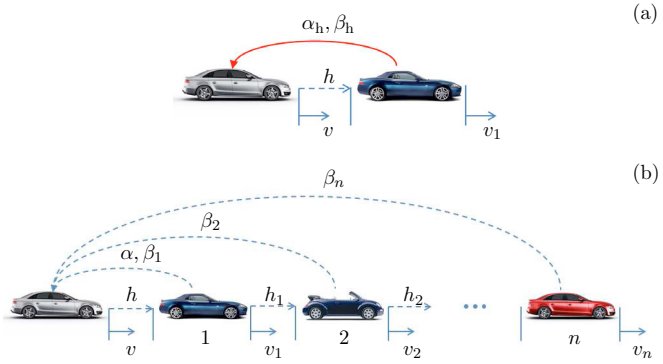

Fig. 1. (a) Human-driven vehicle monitors the vehicle immediately ahead. (b) CCC vehicle at the tail receives information from n vehicles ahead. The velocities and the headways are denoted by $v, v_1, ..., v_n$ and $h, h_1, ..., h_{n-1}$, respectively. The gain parameters are displayed along the communication links.

β_i, $i = 1, ..., n$ are the gains for the velocity differences. We remark that if vehicle i does not broadcast its velocity, we set the corresponding gain $\beta_i = 0$. Finally, Δt represents the sampling period of the digital controller, which is set to be larger than the time needed for sampling, broadcasting, receiving and processing the information. The sampling frequency should satisfy the Nyquist criterion, i.e., $\frac{2\pi}{\Delta t} > 2\omega_{\max}$, where $\omega_{\max}$ is the largest meaningful angular frequency for longitudinal vehicle dynamics. Setting $\Delta t = 0.1$ [s], which is common in V2V communication, the Nyquist criterion is typically satisfied.

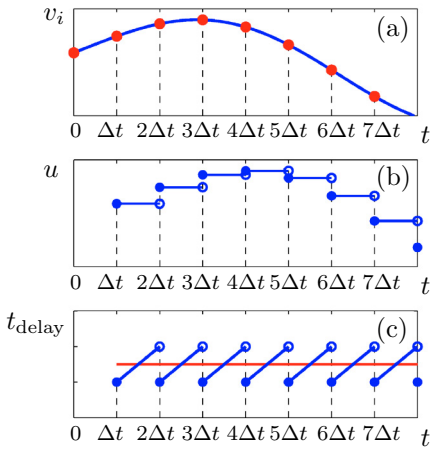

Fig. 2. (a) The velocity of vehicle i (solid blue line) as a function of time with sampled data (red dots). (b) The control signal of a CCC vehicle as a function of time. (c) The change of the delay in the control loop as a function of time, where the average delay is represented by the red horizontal line.

Again, we consider the dynamics about equilibrium

$$h(t) \equiv h^*, \quad v(t) \equiv v_i(t) \equiv v^* = V(h^*), \quad i = 1, ..., n, \tag{11}$$

define the perturbations

$$\begin{aligned}\tilde{h}(t) &= h(t) - h^*, \quad \tilde{v}(t) = v(t) - v^*,\\ \tilde{v}_i(t) &= v_i(t) - v^*, \quad i = 1, ..., n,\end{aligned} \tag{12}$$

and integrate (10) between $k\Delta t$ and $(k+1)\Delta t$ to obtain the linear difference equation

$$x[k+1] = A_{c0}x[k]+A_{c1}x[k-1]+\sum_{i=1}^{n} B_{ci}\tilde{v}_i[k-1]+B_\Delta \quad (13)$$

where $x = \begin{bmatrix}\tilde{h} & \tilde{v}\end{bmatrix}^{\mathrm{T}}$ and the matrices are given by

$$A_{c0} = \begin{bmatrix}1 & -\Delta t\\ 0 & 1\end{bmatrix}, \qquad A_{c1} = \begin{bmatrix}-\frac{1}{2}\alpha N\Delta t^2 & \frac{1}{2}\big(\alpha+\sum_{i=1}^{n}\beta_i\big)\Delta t^2\\ \alpha N\Delta t & -\big(\alpha+\sum_{i=1}^{n}\beta_i\big)\Delta t\end{bmatrix},$$
$$B_{ci} = \begin{bmatrix}-\frac{1}{2}\beta_i\Delta t^2\\ \beta_i\Delta t\end{bmatrix}, \quad B_\Delta = \begin{bmatrix}\int_{k\Delta t}^{(k+1)\Delta t}\tilde{v}_1(t)\mathrm{d}t\\ 0\end{bmatrix}. \quad (14)$$

Again, we are most interested in the longitudinal velocity of the vehicle, so we use the output $\tilde{v}$, cf. (7).

Notice that in (13) velocity of each vehicle ahead is considered as an input. Similarly to the continuous-time system, we can use transfer functions to represent the dynamic relationship between each input and the output. To refer to the network structure on Fig. 1(b), we call these *link transfer functions*.

In particular, the link transfer function $T_i^{\mathrm{c}}(z)$ represents the dynamic relationship between the input $\tilde{v}_i(t)$ and the output $\tilde{v}(t)$ when all other inputs are 0. Taking the Z-transform of (7,13) with zero initial condition, one may obtain

$$\tilde{V}(z) = \sum_{i=1}^{n} T_i^{\mathrm{c}}(z)\tilde{V}_i(z), \quad (15)$$

where $\tilde{V}(z)$ and $\tilde{V}_i(z)$ represent the Z-transform of $\tilde{v}[k]$ and $\tilde{v}_i[k]$, respectively, and

$$T_i^{\mathrm{c}}(z) = \begin{cases} C(zI - A_{c0} - A_{c1}z^{-1})^{-1}\big(B_{c1}z^{-1} + (\tilde{B}_{c0} + \tilde{B}_{c1}z^{-1})\big) & \text{if } i = 1,\\ C(zI - A_{c0} - A_{c1}z^{-1})^{-1}B_{ci}z^{-1} & \text{otherwise.}\end{cases} \quad (16)$$

Again, considering the periodic input $\tilde{v}_i(t) = v_i^{\mathrm{amp}}\sin(\omega t+\phi_i) \Rightarrow \tilde{v}_i[k] = v_i^{\mathrm{amp}}\sin(\omega k\Delta t+\phi_i)$, the steady state output can be obtained by $\tilde{v}^{\mathrm{ss}}[k] = |T_i^{\mathrm{c}}(\mathrm{e}^{\mathrm{j}\omega\Delta t})|v_i^{\mathrm{amp}}\sin(\omega k\Delta t + \phi_i + \measuredangle T_i^{\mathrm{c}}(\mathrm{e}^{\mathrm{j}\omega\Delta t}))$.

As a matter of fact, we already assumed periodic input when defining the matrices $\tilde{B}_{c0}$ and $\tilde{B}_{c1}$ in (16). In particular, plugging $\tilde{v}_1(t) = v_1^{\mathrm{amp}}\sin(\omega t+\phi_1)$ into B_Δ in (14), we have

$$B_\Delta = \begin{bmatrix}\frac{\sin(\omega\Delta t)}{\omega}v_1^{\mathrm{amp}}\sin(\omega k\Delta t+\phi_1) + \frac{1-\cos(\omega\Delta t)}{\omega}v_1^{\mathrm{amp}}\cos(\omega k\Delta t+\phi_1)\\ 0\end{bmatrix}. \quad (17)$$

Using trigonometric identities, $v_1^{\mathrm{amp}}\cos(\omega k\Delta t+\phi_1)$ can be expressed with the help of $\tilde{v}_1[k]$ and $\tilde{v}_1[k-1]$, which yields

$$B_\Delta = \tilde{B}_{c0}\tilde{v}_1[k] + \tilde{B}_{c1}\tilde{v}_1[k-1], \quad (18)$$

where

$$\tilde{B}_{c0} = \begin{bmatrix}\frac{\sin(\omega\Delta t)}{\omega} + \frac{1-\cos(\omega\Delta t)}{\omega\tan(\omega\Delta t)}\\ 0\end{bmatrix}, \quad \tilde{B}_{c1} = \begin{bmatrix}\frac{\cos(\omega\Delta t)-1}{\omega\sin(\omega\Delta t)}\\ 0\end{bmatrix}. \quad (19)$$

2.3 Plant Stability and Head-to-tail String Stability

Plant stability indicates the ability of a vehicle to approach steady state when no disturbances are imposed by other vehicles. For LTI systems, we can evaluate plant stability by the locations of poles of the transfer function. Specifically, for continuous-time LTI systems, all the poles must be on the left half complex plane, while for discrete-time LTI systems, all the poles must be inside the unit circle.

String stability is the ability of a vehicle to attenuate disturbances imposed by the vehicles ahead. To be more specific, in this paper we apply the concept of head-to-tail string stability, which requires that the disturbances of head vehicle are attenuated by the tail vehicle. Note that this definition allows vehicles in the string to increase disturbances, which makes it feasible to evaluate the behavior of connected vehicle systems containing human-driven vehicles whose dynamics cannot be designed.

Fourier's theory states that any periodic signal can be represented as an infinite sum of sinusoidal functions, which can also be extended to any absolutely integrable non-periodic signals. Hence, we assume the head vehicle's velocity to be

$$v_n(t) = v_n^* + v_n^{\mathrm{amp}}\sin(\omega t) \;\Leftrightarrow\; \tilde{v}_n(t) = v_n^{\mathrm{amp}}\sin(\omega t), \quad (20)$$

which results in the steady state velocity response of the tail vehicle

$$\tilde{v}^{\mathrm{ss}}(t) = v^{\mathrm{amp}}\sin(\omega t+\phi), \quad (21)$$

where v^{amp} and ϕ depend on the excitation frequency ω.

Based on the setup above, a vehicle string is head-to-tail string stable if

$$v^{\mathrm{amp}}(\omega) < v_n^{\mathrm{amp}}, \quad \text{for } \forall\omega > 0. \quad (22)$$

For LTI systems, we can use the norm of frequency response function to evaluate string stability:

$$|H(\omega)| = \frac{v^{\mathrm{amp}}(\omega)}{v_n^{\mathrm{amp}}} < 1, \quad (23)$$

where H is a complex number. For continuous-time LTI systems, $H(\omega) = G^{\mathrm{h}}(\mathrm{j}\omega)$, where $G^{\mathrm{h}}(s)$ is the continuous-time head-to-tail transfer function, while for discrete-time LTI systems, $H(\omega) = G^{\mathrm{c}}(\mathrm{e}^{\mathrm{j}\omega\Delta t})$, where $G^{\mathrm{c}}(z)$ is the discrete-time head-to-tail transfer function.

In the following section we will show how to compute $G^{\mathrm{h}}(s)$ and $G^{\mathrm{c}}(z)$ for vehicle systems made of human-driven vehicles and made of CCC vehicles, respectively. Then we will give a method to analyze heterogeneous connected vehicle systems containing both human-driven vehicles and CCC vehicles.

3. STRING STABILITY OF HETEROGENEOUS CONNECTED VEHICLE SYSTEMS

In this section, we discuss head-to-tail string stability for strings of human-driven vehicles and for strings of CCC vehicles. Then, we derive a general formula that allows us to analyze connected vehicle systems that include both human-driven vehicles and CCC vehicles.

3.1 Human-driven Vehicle Network

A human-driven vehicle is modeled as a continuous-time single input single output (SISO) system, cf. (5). When assuming a chain of $(n+1)$ human-driven vehicles with identical drivers, one may use the $T^{\mathrm{h}}(s)$ defined in (9) to describe the dynamical interaction between consecutive vehicles. That is, we may set up a dynamic coupling matrix $\mathbf{T}(s) = [T_{i,k}(s)]$, such that

$$T_{i,k}(s) = \begin{cases}1 & \text{if } i = k,\\ T^{\mathrm{h}}(s) & \text{if } i = k-1,\\ 0 & \text{otherwise,}\end{cases} \quad (24)$$

for $i,k=1,...,n+1$. Or equivalently,

$$\mathbf{T}(s)=\begin{bmatrix}1 & T^{\mathrm{h}}(s) & 0 & \dots & 0\\ 0 & 1 & T^{\mathrm{h}}(s) & \dots & 0\\ 0 & 0 & 1 & \ddots & \vdots\\ \vdots & \vdots & \vdots & \ddots & T^{\mathrm{h}}(s)\\ 0 & 0 & 0 & \dots & 1\end{bmatrix}. \tag{25}$$

According to (Zhang and Orosz, 2016), the head-to-tail transfer function $G^{\mathrm{h}}(s)$ can be calculated by constructing

$$\tilde{\mathbf{T}}(s)=\mathbf{R}_1\mathbf{T}(s)\mathbf{R}_2 \tag{26}$$

where $\mathbf{R}_1=[\mathbf{I}_n,\mathbf{0}_{n\times 1}]$ and $\mathbf{R}_2=[\mathbf{0}_{n\times 1},\mathbf{I}_n]^T$ that correspond to to deleting the first column and last row of $\mathbf{T}(s)$. Then one shall use the determinant with no sign changes

$$G^{\mathrm{h}}(s)=\sum_{\sigma_i\in S_n}\prod_{i=1}^{n}\tilde{T}_{i,\sigma_i}(s)=\left(T^{\mathrm{h}}(s)\right)^n, \tag{27}$$

where the sum is computed over all permutations of the set $S_n=\{1,2,...,n\}$. Indeed, (27) shows that the stability of a human-driven vehicle is equivalent to that of a vehicle chain.

Fig. 3(a) shows the stability chart in the $(\alpha_{\mathrm{h}},\beta_{\mathrm{h}})$ plane for $\tau=0.15[s]$ for a 2-vehicle string where $G^{\mathrm{h}}(s)=T^{\mathrm{h}}(s)$. In the light pink domain only plant stability is guaranteed, while the light blue domain is plant and string stable. To compute the plant stable region, we check that all poles of $T^{\mathrm{h}}(s)$ are located on the left half complex plane, while to compute the string stable region, we check $|T^{\mathrm{h}}(\mathrm{j}\omega)|<1$ for all $\omega>0$; see (Zhang and Orosz, 2016).

3.2 CCC Vehicle Network

A CCC vehicle is represented by a discrete-time multiple inputs single output (MISO) system, cf. (13). For a chain of $(n+1)$ CCC vehicles where each vehicle monitors the motion of all vehicles ahead, we use $T_i^{\mathrm{c}}(z)$ defined in (16) to create the dynamic coupling matrix $\mathbf{T}(z)=[T_{i,k}(z)]$ such that

$$T_{i,k}(z)=\begin{cases}1 & \text{if } i=k,\\ T^{\mathrm{c}}_{k-i}(z) & \text{if } i<k,\\ 0 & \text{otherwise,}\end{cases} \tag{28}$$

which is equivalent to the upper triangular matrix

$$\mathbf{T}(z)=\begin{bmatrix}1 & T_1^{\mathrm{c}}(z) & T_2^{\mathrm{c}}(z) & \dots & T_n^{\mathrm{c}}(z)\\ 0 & 1 & T_1^{\mathrm{c}}(z) & \dots & T^{\mathrm{c}}_{(n-1)}(z)\\ 0 & 0 & 1 & \ddots & \vdots\\ \vdots & \vdots & \vdots & \ddots & T_1^{\mathrm{c}}(z)\\ 0 & 0 & 0 & \dots & 1\end{bmatrix}. \tag{29}$$

Again, the head-to-tail transfer function is given by

$$\tilde{\mathbf{T}}(z)=\mathbf{R}_1\mathbf{T}(z)\mathbf{R}_2, \tag{30}$$

$$G^{\mathrm{c}}(z)=\sum_{\sigma_i\in S_n}\prod_{i=1}^{n}\tilde{T}_{i,\sigma_i}(z), \tag{31}$$

cf. (26,27). Fig. 3(b) shows the stability chart in the (α,β_1) plane for $\Delta t=0.1[s]$ for a 2-vehicle string, where $G^{\mathrm{c}}(z)=T_1^{\mathrm{c}}(z)$. The same notation is used as in Fig. 3(a). To compute the plant stable region, we check that the poles of $T_1^{\mathrm{c}}(z)$ are located inside the unit circle, while to compute the string stable region, we check that $|T_1^{\mathrm{c}}(\mathrm{e}^{\mathrm{j}\omega\Delta t})|<1$ for all $\omega>0$; see (Qin et al., 2015). Notice that Fig. 3(a) and Fig. 3(b) look very similar. Fig. 2(c) explains the reason: the CCC vehicle discrete dynamics can be approximated by a continuous system using the average delay $\tau=\frac{3}{2}\Delta t$.

In order to highlight the difference between the stability charts, we mark point P at $(2.27,4.00)$ in Fig. 3(a) and (b) and plot the corresponding frequency responses on Fig. 3(c) and (d). On panel (c) $H(\omega)=G^{\mathrm{h}}(\mathrm{j}\omega)$ and P is at the string stability boundary, while on panel (d) $H(\omega)=G^{\mathrm{c}}(\mathrm{e}^{\mathrm{j}\omega\Delta t})$ and point P is slightly in the string unstable domain.

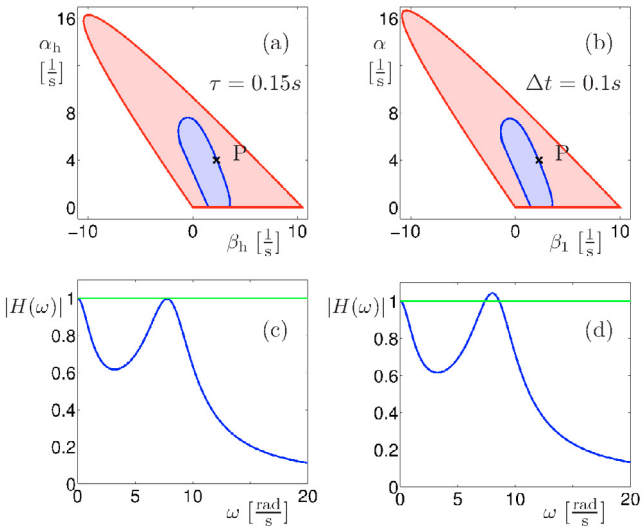

Fig. 3. (a) Stability chart in the $(\alpha_{\mathrm{h}},\beta_{\mathrm{h}})$ plane for a human-driven vehicle. (b) Stability chart in the (α,β_1) plane for a CCC vehicle monitoring one car ahead. (c,d) frequency response at point P.

3.3 Heterogeneous Vehicle Networks

Here we consider a string composed of $(n+1)$ vehicles and assume each vehicle may be either human-driven vehicle or CCC vehicle. For simplicity, we assume all human drivers are identical and all CCC vehicles are driven by the same controller, but the method shown here can be easily extended to handle the cases with higher levels of heterogeneity.

To unify the mathematical description, we compute the Laplace transform of (10) with zero initial condition. In this case the Laplace transform of $\tilde{v}(t)$ can be written as

$$\tilde{V}(s)=\tilde{V}^*(s)\frac{\mathrm{e}^{s\Delta t}(1-\mathrm{e}^{-s\Delta t})^2}{s^2\Delta t}, \tag{32}$$

where the starred transform is given by

$$\tilde{V}^*(s)=\sum_{k=0}^{\infty}\tilde{v}(k\Delta t)\mathrm{e}^{-sk\Delta t}. \tag{33}$$

We can construct a pulse transfer function $T_i^*(s)$ to represent the dynamic relationship between the input $\tilde{v}_i(t)$ and the output $\tilde{v}(t)$ at the sampled instants when all other inputs are 0. That is, similar to (15), we have

$$\tilde{V}^*(s) = \sum_{i=1}^{n} T_i^*(s)\tilde{V}_i^*(s), \tag{34}$$

and (32,34) yields

$$\tilde{V}(s) = \frac{\mathrm{e}^{s\Delta t}(1-\mathrm{e}^{-s\Delta t})^2}{s^2\Delta t}\sum_{i=1}^{n} T_i^*(s)\tilde{V}_i^*(s). \tag{35}$$

For a complex function $W(s)$ one may use the Residual Theorem to directly calculate

$$W^*(s) = \sum_i \mathrm{Res}\Big(\frac{W(\lambda)}{1-\mathrm{e}^{-(s-\lambda)\Delta t}}, p_i\Big) = \sum_i \frac{1}{(m_i-1)!}\frac{\mathrm{d}^{(m_i-1)}}{\mathrm{d}\lambda^{(m_i-1)}}\Big(\frac{(\lambda-p_i)^{m_i}W(\lambda)}{1-\mathrm{e}^{-(s-\lambda)\Delta t}}\Big)\Big|_{\lambda=p_i},$$

where the sum is over the poles p_i of $W(s)$ and m_i denotes the algebraic multiplicity of the pole p_i. Note that the starred transform has the following three properties:

- $W^*(s) = W(z)|_{z=\mathrm{e}^{s\Delta t}}$;
- $\big(W_1(s)W_2^*(s)\big)^* = W_1^*(s)W_2^*(s)$;
- $\big(\mathrm{e}^{-sk\Delta t}W(s)\big)^* = \mathrm{e}^{-sk\Delta t}W^*(s)$.

The proofs of these are given in (Phillips and Nagle, 2007).

Now we can construct a head-to-tail pulse transfer function that can be used to calculate the steady state velocity response of the tail vehicle imposed by the velocity fluctuation of the head vehicle at the sampled instants. For a vehicle string of $(n+1)$ vehicles, we can use the adjacency matrix $\mathbf{\Gamma} = [\gamma_{i,k}]$ to represent the connectivity structure, where

$$\gamma_{i,k} = \begin{cases} 1 & \text{if vehicle } (i-1) \text{ utilizes data of vehicle } (k-1), \\ 0 & \text{otherwise.} \end{cases} \tag{36}$$

Since each vehicle only utilizes the motion information of vehicles ahead, $\mathbf{\Gamma}$ is an upper triangular matrix.

We define the dynamic coupling matrix $\mathbf{T}(s,z) = [T_{i,k}]$, where

$$T_{i,k} = \begin{cases} \gamma_{i,k}T_{i,k}(s) & \text{if vehicle } (i-1) \text{ is human} - \text{driven}, \\ \gamma_{i,k}T_{i,k}(z) & \text{if vehicle } (i-1) \text{ is CCC}, \end{cases} \tag{37}$$

and the modified dynamic coupling matrix

$$\tilde{\mathbf{T}}(s,z) = \mathbf{R}_1\mathbf{T}(s,z)\mathbf{R}_2, \tag{38}$$

cf. (26,30). Now we define a link operator $\otimes$ to indicate the cascading structure of subsystems:

- $T_{a,b}(s) \otimes T_{b,c}(s) = T_{a,b}(s)T_{b,c}(s) := T_{a,c}(s)$;
- $T_{a,b}(z) \otimes T_{b,c}(s) \otimes T_{c,d}(z) = T_{a,b}(z)\Big(\frac{\mathrm{e}^{s\Delta t}(1-\mathrm{e}^{-s\Delta t})^2}{s^2\Delta t}T_{b,c}(s)\Big)^*\Big|_{s=\frac{\ln(z)}{\Delta t}} T_{c,d}(z).$

Note that $\otimes$ is not commutative.

Then we can calculate the head-to-tail pulse transfer function by

$$G(s,z) = \sum_{\sigma_i \in S_n} \bigotimes_{i=1}^{n} \tilde{T}_{i,\sigma_i} \tag{39}$$

where the ordered product is given by

$$\bigotimes_{i=1}^{n} \tilde{T}_{i,\sigma_i} = \tilde{T}_{1,\sigma_i} \otimes \tilde{T}_{2,\sigma_i} \otimes \cdots \otimes \tilde{T}_{n,\sigma_i}, \tag{40}$$

and the sum in (39) is computed over all permutations of the set $S_n = \{1, 2, ..., n\}$, cf. (27,31).

For example,

$$T_{0,1}(z) \otimes T_{1,2}(s) \otimes T_{2,3}(s) \otimes T_{3,5}(z) = T_{0,1}(z)\Big(\frac{\mathrm{e}^{s\Delta t}(1-\mathrm{e}^{-s\Delta t})^2}{s^2\Delta t}T_{1,2}(s)T_{2,3}(s)\Big)^*\Big|_{s=\frac{\ln(z)}{\Delta t}} T_{3,5}(z). \tag{41}$$

Formula (39) yields the head-to-tail frequency response

$$H(\omega) = G(\mathrm{j}\omega, \mathrm{e}^{\mathrm{j}\omega\Delta t}). \tag{42}$$

To be consistent with (37) and (39), for vehicle $(i-1)$ in the string we can generalize (14) as

$$A_{\mathrm{c1}} = \begin{bmatrix} -\frac{1}{2}\alpha N\Delta t^2 & \frac{1}{2}\big(\alpha + \sum_{k=i+1}^{n+1}\gamma_{i,k}\beta_{k-i}\big)\Delta t^2 \\ \alpha N\Delta t & -\big(\alpha + \sum_{k=i+1}^{n+1}\gamma_{i,k}\beta_{k-i}\big)\Delta t \end{bmatrix} \tag{43}$$

4. CASE STUDIES

To represent the construction above, we provide two case studies. First, we look at a vehicle string composed of 3 vehicles shown in Fig. 4: vehicle 0 at the tail and vehicle 2 at the head are CCC vehicles, while vehicle 1 in the middle is human-driven. Also, we compare the exact frequency response of this system derived from our approach to those obtained by discrete-time approximation and continuous-time approximation.

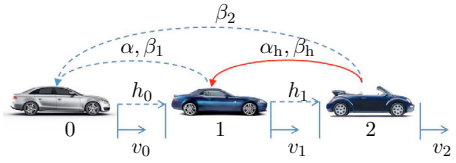

Fig. 4. Vehicle string model composed of 3 vehicles. Blue dashed links indicate digital control, while red continuous link indicates continuous-time control.

By applying (36-42), one can show that the amplitude ratio of $v_0(t)$ and $v_2(t)$ is given by $|H(\omega)|$, where

$$H(\omega) = G(\mathrm{j}\omega, e^{\mathrm{j}\omega\Delta t}) = T_2^{\mathrm{c}}(e^{\mathrm{j}\omega\Delta t}) + T_1^{\mathrm{c}}(e^{\mathrm{j}\omega\Delta t})\Big(\frac{e^{s\Delta t}(1-e^{-s\Delta t})^2}{s^2\Delta t}T^{\mathrm{h}}(s)\Big)^*\Big|_{s=\mathrm{j}\omega} \tag{44}$$

Note that $T^{\mathrm{h}}(s)$ has infinitely many poles, cf. (9). When applying the Residual Theorem, we use DDE-BIFTOOL (Engelborghs et al., 2001) to compute the leading poles numerically. In fact, using the leading 3 poles and using the leading 20 poles give very close results.

In Fig. 5 solid blue curves indicate $|H(\omega)|$ in case of sampling time $\Delta t = 0.1$ [s], human reaction time $\tau = 0.45$ [s] and human gains $\alpha_\mathrm{h} = 0.6$ [1/s], $\beta_\mathrm{h} = 0.9$ [1/s] for different values of α, β_1, β_2 as indicated. We compare these to the results of two different approximations. Dashed red curves represent the case when the discrete dynamics of the CCC vehicle is approximated by continuous time system containing the average delay $\tau = \frac{3}{2}\Delta t = 0.15$ [s]; see Fig. 2(c). On the other hand, dotted green curves represent the case when the constant human reaction time is substituted with time varying delay similar to those in Fig. 2(c) but with minimum value $4\Delta t = 0.4$ [s] and maximum value $5\Delta t = 0.5$ [s]. Observe that

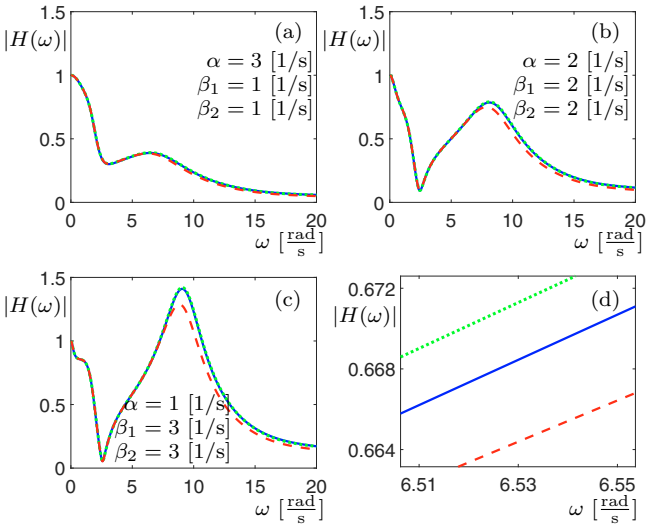

Fig. 5. (a,b,c) Frequency response (44) for human delay $\tau = 0.45$ [s], human gains $\alpha_{\rm h} = 0.6$ [1/s], $\beta_{\rm h} = 0.9$ [1/s], and sampling time $\Delta t = 0.1$ [s] and different values of gain parameters as indicated, corresponding to the system in Fig. 5. Solid blue curves correspond to the exact $H(\omega)$, while dashed red curves correspond to the continuous-time approximation and dotted green curves to the discrete-time approximation.

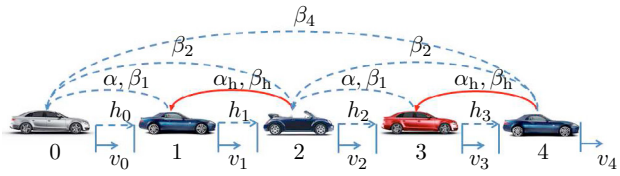

Fig. 6. Vehicle string model composed of 5 vehicles. Blue dashed links indicate digital control, while red continuous links indicate continuous-time control.

the approximations capture the real case well. The small differences are shown by the zoom in Fig. 5(d).

Now we consider a more complex vehicle network and analyze the string stable domain of the control gains. Fig. 6 show a string where vehicles 0, 2, 4 are CCC vehicles, while vehicles 1, 3 are human-driven vehicles.

By applying (39), we obtain

$$\begin{aligned} H(\omega) &= G(\mathrm{j}\omega, e^{\mathrm{j}\omega\Delta t}) \qquad (45)\\ &= T_4^{\rm c}(e^{\mathrm{j}\omega\Delta t}) + \left(T_2^{\rm c}(e^{\mathrm{j}\omega\Delta t})\right)^2 \\ &+ \left(T_1^{\rm c}(e^{\mathrm{j}\omega\Delta t})\right)^2 \Big(\big(\frac{e^{s\Delta t}(1-e^{-s\Delta t})^2}{s^2\Delta t} T^{\rm h}(s) \big)^* \Big|_{s=\mathrm{j}\omega} \Big)^2 \\ &+ 2T_1^{\rm c}(e^{\mathrm{j}\omega\Delta t}) T_2^{\rm c}(e^{\mathrm{j}\omega\Delta t}) \big(\frac{e^{s\Delta t}(1-e^{-s\Delta t})^2}{s^2\Delta t} T^{\rm h}(s) \big)^* \Big|_{s=\mathrm{j}\omega}. \end{aligned}$$

Here we use our method to design the gains β_1 and β_2 while fixing the human parameters as $\tau = 0.45$ [s], $\alpha_{\rm h} = 0.6$ [1/s], $\beta_{\rm h} = 0.9$ [1/s] and the other parameters as $\Delta t = 0.1$ [s], $\alpha = 0.6$ [1/s] and $\beta_4 = 0$. In the blue shaded domain shown in Fig. 7, the string stability condition (23) is satisfied.

5. CONCLUSIONS

In this paper we proposed a method to obtain the steady state dynamics of heterogeneous connected vehicle systems containing CCC vehicles that are controlled in discrete time and human-driven vehicles that are controlled in continuous time. The proposed approach allowed us to evaluate the head-to-tail string stability for complex vehicle networks in an efficient manner. It also serves as a benchmark to justify the analyses conducted by two approximation methods discussed in this paper.

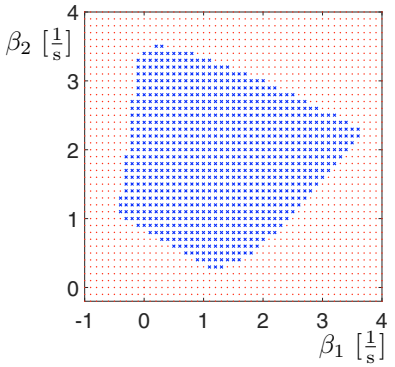

Fig. 7. Stability chart for string in Fig. 6.

ACKNOWLEDGEMENTS

The authors acknowledge discussions with Jin Ge, Wubing Qin and Linjun Zhang. This work was supported by the National Science Foundation (Award No. 1300319).

REFERENCES

Alam, A., Mårtensson, J., and Johansson, K.H. (2015). Experimental evaluation of decentralized cooperative cruise control for heavy-duty vehicle platooning. *Control Engineering Practice*, 38, 11–25.

di Bernardo, M., Salvi, A., and Santini, S. (2015). Distributed consensus strategy for platooning of vehicles in the presence of time-varying heterogeneous communication delays. *IEEE Transactions on Intelligent Transportation Systems*, 16(1), 102–112.

Engelborghs, K., Luzyanina, T., and Samaey, G. (2001). DDE-BIFTOOL v. 2.00: a matlab package for bifurcation analysis of delay differential equations.

Ge, J.I. and Orosz, G. (2014). Dynamics of connected vehicle systems with delayed acceleration feedback. *Transportation Research Part C*, 46, 46–64.

Kianfar, R., Augusto, B., Ebadighajari, A., Hakeem, U., Nilsson, J., Raza, A., Tabar, R.S., Irukulapati, N.V., Englund, C., Falcone, P., Papanastasiou, S., Svensson, L., and Wymeersch, H. (2012). Design and experimental validation of a cooperative driving system in the grand cooperative driving challenge. *IEEE Transactions on Intelligent Transportation Systems*, 13(3), 994–1007.

Orosz, G. (2014). Connected cruise control: modeling, delay effects, and nonlinear behavior. *Vehicle System Dynamics*, (submitted).

Phillips, C.L. and Nagle, H.T. (2007). *Digital control system analysis and design*. Prentice Hall Press.

Qin, W.B., Gomez, M.M., and Orosz, G. (2015). Stability and frequency response under stochastic communication delays with applications to connected cruise control design. In *IEEE Transactions on Intelligent Transportation Systems*, (submitted).

Zhang, L. and Orosz, G. (2016). Motif-based design for connected vehicle systems in presence of heterogeneous connectivity structures and time delays. *IEEE Transactions on Intelligent Transportation Systems*, (accepted).